Acta Pharm. Sci. Vol 64:(4), 2026
Original article
DOI: 10.23893/1307-2080.APS64030

OPEN ACCESS

Differential apoptosis-associated responses of neurons and glial cells to cisplatin in primary cortical cultures

Neşe AYŞİT[1,2,3*], Ayça ÖNAL[1,2,3], Esra ALTINTAŞ[1,2,3], Arda KEBAPÇI[1,2,3]

1 İstanbul Medipol University, Regenerative and Restorative Medicine Research Center (REMER), Research Institute for Health Sciences and Technologies (SABITA), İstanbul, Türkiye

2 İstanbul Medipol University, Graduate School of Health Sciences, Istanbul, Türkiye

3 İstanbul Medipol University, School of Medicine, Department of Medical Biology, Istanbul, Türkiye

ABSTRACT

Cisplatin is a platinum-based chemotherapeutic agent widely used to treat solid tumors; however, its clinical use is limited by severe neurotoxicity. Although cisplatin shows limited blood–brain barrier permeability, accumulating evidence indicates that it induces apoptosis-associated neurotoxicity in the central nervous system. In this study, we investigated cell type–specific apoptosis-associated responses of primary cortical neurons and glial cells to cisplatin. Cytotoxicity was evaluated in EMT6 murine mammary carcinoma cells using the 3-(4,5-dimethylthiazol-2-yl)-2,5-diphenyltetrazolium bromide (MTT) assay, and the half-maximal inhibitory concentration (IC_{50}) was determined. This concentration was then applied to primary cortical cultures derived from postnatal day 0 Balb/C mice. Apoptosis-associated responses were assessed by Western blot analysis of BCL-2 expression and immunofluorescence staining of caspase-3. Cisplatin significantly reduced BCL-2 protein levels in primary cortical cultures ($p<0.01$). Immunofluorescence analysis further revealed a significant increase in caspase-3–positive neurons following cisplatin exposure ($p<0.01$), whereas no significant change was observed in GFAP-positive glial cells ($p>0.05$). These findings demonstrate that cisplatin induces cell type–specific apoptosis-associated

* Corresponding author: Neşe AYŞİT
E-mail: naysit@medipol.edu.tr
ORCIDS:
Neşe AYŞİT: 0000-0002-4243-9092
Ayça ÖNAL: 0009-0002-7723-8378
Esra ALTINTAŞ: 0000-0002-7622-0152
Arda KEBAPÇI: 0000-0003-0556-8247
(Received 21 Feb 2026, Accepted 27 Apr 2026)

Acta Pharmaceutica Sciencia is licensed under a Creative Commons Attribution-NonCommercial-NoDerivatives 4.0 International License.
© Medipol University Press / e-ISSN: 1307-2080

responses in primary cortical cultures, with neurons showing greater vulnerability than glial cells, highlighting the importance of evaluating cisplatin-induced neurotoxicity in the central nervous system.

Keywords: cisplatin, neurotoxicity, apoptosis, caspase 3, cerebral cortex

INTRODUCTION

Cancer remains one of the leading causes of morbidity and mortality worldwide[1]. Despite major advances in targeted therapies, chemotherapy continues to represent a cornerstone of treatment for many malignancies[2]. However, chemotherapy-induced neurotoxicity is a well-documented adverse effect that manifests as peripheral neuropathy and cognitive impairment in a substantial proportion of patients[3,4].

Cisplatin is a platinum-based chemotherapeutic agent that is extensively used in the management of various solid tumors owing to its potent cytotoxic effects, which are primarily mediated through DNA crosslinking and the induction of apoptosis[5-7]. Nevertheless, the clinical utility of cisplatin is substantially constrained by severe adverse effects, particularly neurotoxicity and ototoxicity[8-11].

The EMT6 cell line, derived from murine mammary carcinoma, represents a well-established experimental model for evaluating the efficacy of anticancer agents[12]. The cytotoxic effects of cisplatin on EMT6 cells can be quantitatively assessed using the MTT assay, a widely accepted colorimetric method that measures cell viability based on mitochondrial metabolic activity[13]. Determination of the IC_{50} value of cisplatin in EMT6 cells provides a valuable reference for estimating its effective concentration for subsequent experimental applications.

Beyond its antitumor efficacy, cisplatin has been implicated in chemotherapy-related cognitive impairment, despite its limited ability to directly cross the blood–brain barrier[14-16]. Emerging evidence indicates that cisplatin induces sustained disruption of blood–brain barrier integrity through cerebrovascular endothelial damage, leading to increased permeability and subsequent neuroinflammation[14,16,17]. These neurotoxic effects are closely associated with oxidative stress, mitochondrial dysfunction, and activation of apoptotic pathways, ultimately compromising neuronal survival and cognitive function[18-21].

Given the heightened vulnerability of the developing brain to such insults, investigating the effects of cisplatin on cortical neurons is of considerable importance for elucidating its potential risks in clinical contexts. In the

present study, we first determined the cytotoxic effects of cisplatin in EMT6 breast cancer cells using the MTT assay and calculated the IC_{50} value. This concentration was subsequently applied to primary cortical cultures derived from postnatal day 0 Balb/C mice to evaluate cisplatin-induced apoptotic progression in neurons of the central nervous system using Western blot and immunofluorescence staining techniques.

METHODOLOGY

Cell culture of EMT6 cells and primary cortical neurons

The murine mammary carcinoma cell line EMT6 (ATCC® CRL-2755™) was cultured in RPMI-1640 medium (Thermo Scientific, #11875093) supplemented with 10% fetal bovine serum (FBS; Gibco, #A5669801) and 50 μg/mL penicillin/streptomycin. Cells were maintained at 37°C in a humidified atmosphere containing 5% CO_2 and were subcultured upon reaching 80–90% confluency. For cytotoxicity assays, cells were detached using trypsin-EDTA (Gibco, #25200056) and seeded into 96-well plates (Corning) at a density of 5×10^3 cells per well. Primary cortical neuron cultures were prepared from postnatal day 0 (P0) neonatal Balb/C mice**.** A total of 10 neonatal mice were used for the preparation of primary cortical cultures (n=5 per group). Briefly, cerebral cortices were carefully dissected and incubated in L-15 medium (Gibco, #11415064) containing papain enzyme (1 mg/mL) at 4°C for 45 minutes to allow gentle enzymatic dissociation. Following enzymatic digestion, tissues were washed with Hank's Balanced Solution (HBSS; Gibco, #24020117), gently triturated using fire-polished Pasteur pipettes to obtain a single-cell suspension, and centrifuged at 1,000 rpm for 5 minutes. The resulting cell pellet was resuspended and seeded onto poly-D-lysine–coated 96-well plates (0.1 mg/mL) at a density of 5×10^3 cells per well. Neuronal cultures were maintained in Neurobasal medium (NBA; Gibco, #10888022) supplemented with 1% B-27 (Gibco, #17504044) and 1% penicillin/streptomycin at 37°C in a humidified atmosphere containing 5% CO_2. Culture medium was partially replaced every 2–3 days.

Cisplatin treatment

24 hours after seeding, EMT6 cells were treated with cisplatin at varying concentrations (10, 20, 50, and 100 μM), along with a vehicle-treated control group. Primary cortical cultures were exposed only to the IC_{50} concentration of cisplatin determined in EMT6 cells.

MTT cell viability assay

Cell viability was assessed using the 3-(4,5-dimethylthiazol-2-yl)-2,5-diphenyltetrazolium bromide (MTT) assay. 24 hours after seeding, EMT6 cells

were treated with cisplatin at the concentrations described in the previous section. Primary cortical neurons were exposed only to the IC_{50} concentration determined in EMT6 cells. Following 48 hours of cisplatin treatment, 10 μL of MTT solution (5 mg/mL in phosphate-buffered saline [PBS]; Thermo Scientific, #M6494) was added to each well and incubated at 37°C in a humidified atmosphere containing 5% CO_2 for 3–4 hours. Subsequently, the MTT-containing medium was carefully removed, and the resulting formazan crystals were dissolved in 200 μL of dimethyl sulfoxide (DMSO, Sigma, #D2650). Absorbance was measured at 570 nm using a microplate reader.

Western blot analysis

Cortical cells exposed only to the IC_{50} concentration determined in EMT6 cells were lysed using RIPA buffer (Thermo Scientific, #89900) supplemented with a protease inhibitor cocktail (Thermo Scientific, #78429). Cell lysates were centrifuged at 20,000 rpm at 4°C for 20 minutes, and the supernatants were collected. Protein concentrations were determined using a NanoDrop spectrophotometer. Equal amounts of protein (30 μg) were separated on 12% polyacrylamide gels and transferred onto polyvinylidene difluoride (PVDF) membranes (Bio-Rad, #16020177). Membranes were blocked with 1% bovine serum albumin (BSA; Sigma, #A9647) prepared in Tris-buffered saline containing 0.1% Tween-20 (TBS-T) for 1 hour at room temperature. Following blocking, membranes were incubated overnight at 4°C with the following primary antibodies: anti-BCL-2 (mouse monoclonal antibody, 1:1000 dilution, Cell Signaling, #2876) and anti-β-actin (mouse monoclonal antibody, 1:1000 dilution, Santa Cruz Biotechnology, #47778). After primary antibody incubation, membranes were washed three times with TBS-T for 5 minutes each and then incubated with horseradish peroxidase (HRP)-conjugated secondary antibodies (goat anti-mouse IgG, 1:2000, Cell Signaling Technology, #ab6789). Following secondary antibody incubation, membranes were washed again three times with TBS-T, and protein bands were visualized using an enhanced chemiluminescence (ECL) detection system (Bio-Rad, #1705061) according to the manufacturer's instructions. Band intensities were quantified using ImageJ software.

Immunofluorescence staining

Immunocytochemical fluorescence staining was performed on cultured cortical neurons following 48 hours of cisplatin treatment. Cells were fixed with 4% paraformaldehyde (PFA; Sigma-Aldrich, #30525-89-4) and subsequently blocked with 5% bovine serum albumin (BSA) containing 0.2% Triton X-100

in phosphate-buffered saline (PBS) for 1 hour at room temperature. Cells were then incubated overnight at 4°C with the following primary antibodies: rabbit monoclonal anti-caspase-3 (Cell Signaling Technology, #9662; 1:500), mouse monoclonal anti-GFAP (Cell Signaling Technology, #3670; 1:500), and mouse anti-β-III-tubulin antibody (Abcam, ab7751; 1:500). After overnight incubation, primary antibodies were removed and cells were washed three times with PBS containing 0.2% Triton X-100 for 5 minutes each. Cells were then incubated with Alexa Fluor–conjugated secondary antibodies (goat anti-rabbit Alexa Fluor 488 (Invitrogen, #710369, 1:500) and goat anti-mouse Alexa Fluor 594 (Invitrogen, #A11032, 1:500)) for 1 hour at room temperature in the dark. Nuclei were counterstained with 4′,6-diamidino-2-phenylindole (DAPI; 1 μg/mL, Sigma-Aldrich, #D9542). Fluorescent images were acquired using a Zeiss LSM 780 confocal microscope equipped with a 20× objective.

Quantification of immunofluorescence signals

Quantitative analysis of caspase-3 immunoreactivity was performed using ZEN Blue software (Zeiss). Cells displaying distinct caspase-3 immunoreactivity localized to the nucleus, together with nuclear condensation or fragmentation as assessed by DAPI staining, and exhibiting pronounced morphological alterations (such as axonal retraction in neurons or structural disruption in glial cells), were considered to exhibit apoptosis-associated features. The percentage of apoptosis-associated neurons was calculated relative to the total number of βIII-tubulin–positive neurons. Glial cells were analyzed separately based on GFAP immunoreactivity.

Statistical analysis

All experiments were performed with three independent biological replicates (n=3), each derived from separate primary cortical cultures. Data are presented as mean ± SEM. Normality was assessed using the Shapiro–Wilk test. Statistical comparisons between two groups were performed using Welch's t-test. A p-value<0.05 was considered statistically significant.

RESULTS and DISCUSSION

Dose-dependent cytotoxic effect of cisplatin in EMT6 cells

To determine an effective experimental concentration for subsequent neuronal analyses, EMT6 murine mammary carcinoma cells were treated with increasing concentrations of cisplatin (10, 20, 50, and 100 μM) for 48 hours, and cell viability was assessed using the MTT assay (Figure 1). Cisplatin treatment resulted in a dose-dependent reduction in cell viability. While 10 μM caused a modest decrease,

concentrations ≥20 μM produced a marked decline in viability accompanied by morphological alterations, including cell shrinkage and partial detachment (Figure 1). The IC_{50} values were calculated as 26 μM using nonlinear regression analysis in GraphPad Prism software (n=3).

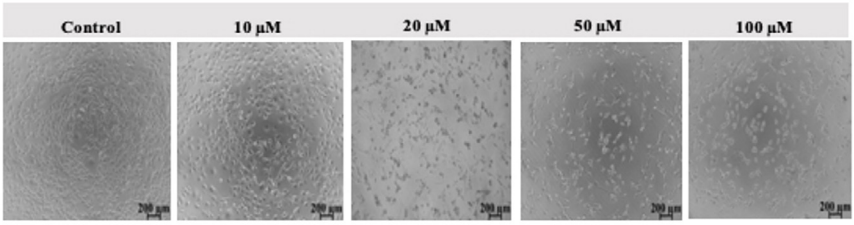

Figure 1. Dose-dependent cytotoxic effects of cisplatin on EMT6 breast cancer cells. Representative phase-contrast images of EMT6 cells treated with increasing concentrations of cisplatin (10, 20, 50, and 100 μM) for 48 hours, compared with untreated control cells. Increasing cisplatin concentrations were associated with a reduction in cell density and observable morphological alterations, including cell shrinkage and partial detachment, indicating a dose-dependent cytotoxic effect. The half-maximal inhibitory concentration (IC_{50}) of cisplatin in EMT6 cells was calculated as 26 μM based on MTT assay results. Scale bar=200 μm.

Cisplatin is widely used in the treatment of solid tumors, including breast cancer, due to its DNA crosslinking and apoptosis-inducing effects[2,5]. Although its neurotoxicity has traditionally been attributed to peripheral nervous system damage[8,9], increasing evidence suggests central nervous system involvement[4,18]. Therefore, the IC_{50} concentration (26 μM) was selected to model clinically relevant exposure conditions in primary cortical cultures.

Cisplatin reduces BCL-2 expression in primary cortical cultures

To evaluate apoptosis-associated molecular alterations in cortical cultures, BCL-2 protein expression was analyzed by Western blot after 48 hours treatment with 26 μM cisplatin (Figure 2). Cisplatin exposure significantly reduced BCL-2 expression compared with control cultures (***$p<0.01$) (Figure 2). β-Actin was used as a loading control. Since protein lysates were obtained from mixed primary cortical cultures containing both neurons and glial cells, this decrease reflects a global reduction in anti-apoptotic signaling within the culture system.

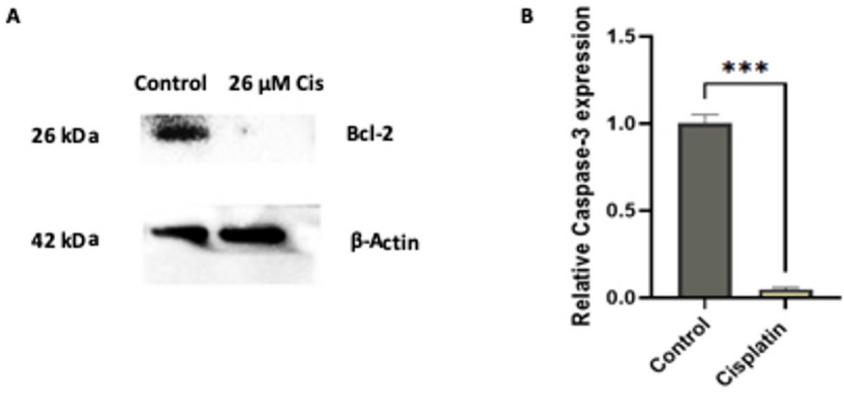

Figure 2. BCL-2 expression in cisplatin-treated primary cortical cultures. (A) Western blot analysis of BCL-2 protein expression in control and cisplatin-treated primary cortical cultures. Cells were treated with 26 µM cisplatin for 48 hours. Protein extracts were separated on a 12% SDS–polyacrylamide gel and immunoblotted as described above. β-Actin was used as a loading control. (B) Data are presented as mean ± SEM of independent experiments (***$p<0.01$, cisplatin vs. control).

Downregulation of BCL-2 is a hallmark of intrinsic (mitochondrial) apoptotic pathway activation[29,30]. Cisplatin-induced mitochondrial dysfunction and oxidative stress have been well documented in neuronal systems[18-20, 31]. Neurons are particularly vulnerable to mitochondrial impairment due to their high dependence on oxidative phosphorylation and limited metabolic reserve[22-24,32,33]. Thus, the observed decrease in BCL-2 suggests activation of apoptosis-associated mechanisms in cortical cultures.

However, Western blot analysis does not identify which cell type primarily contributes to this reduction. Therefore, cell type–specific immunofluorescence analyses were performed.

Cisplatin induces caspase-3 activation in βiii-tubulin–positive neurons

To determine whether neurons exhibit apoptosis-associated changes following cisplatin exposure, caspase-3 immunoreactivity was analyzed in βIII-tubulin–positive cortical neurons (Figure 3). Cisplatin treatment resulted in a significant increase in the percentage of neurons displaying nuclear caspase-3 immunoreactivity and morphological features consistent with apoptosis, including nuclear condensation and neurite retraction (**$p<0.01$) (Figure 3).

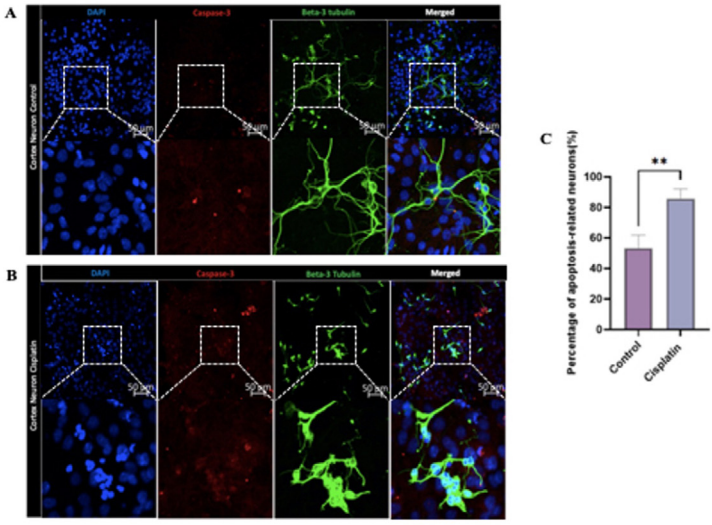

Figure 3. Cisplatin treatment significantly increases caspase-3 immunoreactivity in β-III tubulin–positive cortical neurons. Representative confocal immunofluorescence images of primary cortical neurons in control (A) and cisplatin-treated (B) groups are shown. Cells were stained with DAPI (blue) to visualize nuclei, caspase-3 (red) as an apoptosis-associated marker, and β-III tubulin (green) to identify neurons. Dashed boxes indicate regions shown as zoomed-in, cropped regions from the same original images to improve visualization. (C) Quantitative analysis demonstrates a significant increase in the percentage of caspase-3-positive β-III tubulin-expressing neurons following cisplatin treatment compared to control cultures. Data are presented as mean ± SEM from three independent cultures (n=3). Statistical analysis was performed using Welch's t-test; **p<0.01. Scale bar=50 µm.

Caspase-3 is a key executioner protease in apoptotic signaling and represents an indicator of irreversible neuronal injury. Previous studies have demonstrated that cisplatin-induced neuronal toxicity involves caspase-3–dependent mechanisms[25-27]. Notably, cisplatin toxicity in the developing brain has been shown to require caspase-3 activation[25]. Our findings are consistent with these reports and indicate that the global reduction in BCL-2 expression (Figure 2) is predominantly driven by neuronal apoptosis.

GFAP-positive glial cells exhibit relative resistance to cisplatin

In contrast to neurons, quantitative analysis revealed no statistically significant increase in apoptosis-associated features in GFAP-positive glial cells following cisplatin treatment (ns) (Figure 4). Furthermore, direct comparison within cisplatin-treated cultures demonstrated significantly greater susceptibility of neurons compared with glial cells (**p<0.01).

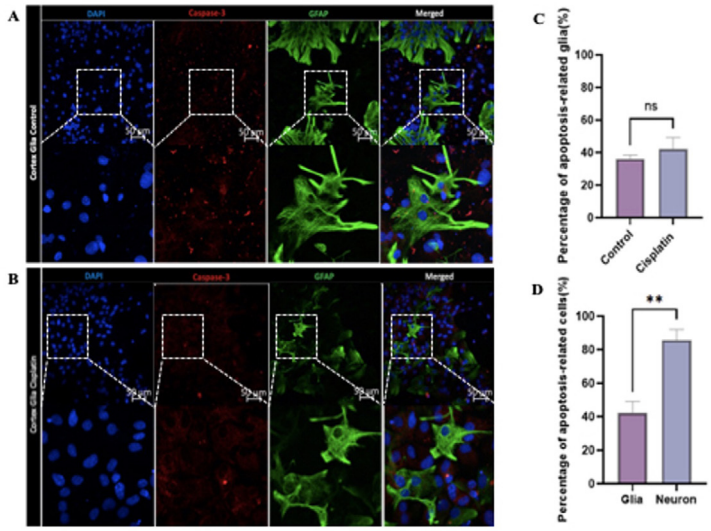

Figure 4. Cisplatin treatment does not significantly affect caspase-3 immunoreactivity in GFAP-positive glial cells. Representative confocal immunofluorescence images of primary cortical glial cells in control (A) and cisplatin-treated (B) groups. Cells were stained with DAPI (blue) to visualize nuclei, caspase-3 (red) as an apoptosis-associated marker, and GFAP (green) to identify glial cells. Dashed boxes indicate regions shown as zoomed-in, cropped regions from the same original images to improve visualization. (C) Quantitative analysis demonstrates no significant difference in the percentage of GFAP-positive glial cells exhibiting caspase-3 immunoreactivity following cisplatin treatment compared to control cultures (ns). (D) Comparison of apoptosis-associated features between neurons and glial cells following cisplatin treatment, showing a significantly higher susceptibility in neurons. Data are presented as mean ± SEM from three independent cultures (n=3). Statistical analysis was performed using Welch's t-test; $p<0.01$ for neurons vs glial cells. Scale bar=50 μm.

The relative resistance of glial cells may be attributed to their stronger antioxidant capacity and glutathione metabolism[25,28], as well as enhanced stress-response mechanisms. Indeed, astrocytes have been reported to protect neurons from cisplatin-induced injury through mitochondrial transfer[14]. However, *in vivo* studies demonstrate that persistent blood–brain barrier disruption following cisplatin exposure may enhance neuronal vulnerability[17].

Taken together, these findings demonstrate a clear cell type–dependent response to cisplatin exposure, with cortical neurons exhibiting significantly greater apoptosis-associated changes compared with glial cells.

In summary, the present study demonstrates that cisplatin induces apoptosis-associated alterations in primary cortical cultures in a cell type–dependent manner. Neurons exhibit significantly greater vulnerability compared to glial cells

under the applied conditions. These findings contribute to the understanding of central nervous system toxicity associated with cisplatin treatment and highlight the importance of evaluating neuronal-specific responses in chemotherapeutic neurotoxicity studies.

STATEMENTS OF ETHICS

The animal study protocol was approved by the Istanbul Medipol University Animal Experiments Ethics Committee (Approval No: 61, Date: 24.10.2024). All experimental procedures were conducted in accordance with institutional and international guidelines for the care and use of laboratory animals, and a total of 10 mice were used in this study.

CONFLICT OF INTEREST STATEMENT

The authors have no conflicts of interest to declare.

AUTHOR CONTRIBUTIONS

Design: NA; acquisition of data: NA, AO, EA; analysis of data: NA, AO; drafting of the manuscript: NA, AK; critical revision of the manuscript: NA, AO, EA, AK; statistical analysis: AO; cell culture and primary experiments: NA; cell-line experiments and drug optimization: EA; imaging and imaging analysis: AO; supervision: NA.

FUNDING SOURCES

This research received no specific grant from any funding agency in the public, commercial, or not-for-profit sectors.

ACKNOWLEDGMENTS

The authors have no acknowledgments.

REFERENCES

1. Sung H, Ferlay J, Siegel RL, Laversanne M, Soerjomataram I, Jemal A, et al. Global cancer statistics 2020: GLOBOCAN estimates of incidence and mortality worldwide for 36 cancers in 185 countries. CA Cancer J Cli, 2021;71(3):209–249. Doi: 10.3322/caac.21660

2. Smolarz B, Nowak AZ, Romanowicz H. Breast cancer—epidemiology, classification, pathogenesis and treatment (review of literature). Cancers, 2022;14(10):2569. Doi: 10.3390/cancers14102569

3. Seretny M, Currie GL, Sena ES, Ramnarine S, Grant R, MacLeod MR, et al. Incidence, prevalence, and predictors of chemotherapy-induced peripheral neuropathy: a systematic review and meta-analysis. Pain, 2014;155(12):2461–2470. Doi: 10.1016/j.pain.2014.09.020

4. Ahles TA, Root JC. Cognitive effects of cancer and cancer treatments. Annu Rev Clin Psychol, 2018;14:425–451. Doi: 10.1146/annurev-clinpsy-050817-084903

5. Smith IE, Talbot DC. Cisplatin and its analogues in the treatment of advanced breast cancer: a review. Br J Cancer, 1992;65(6):787–793. Doi: 10.1038/bjc.1992.169

6. Dasari S, Tchounwou PB. Cisplatin in cancer therapy: molecular mechanisms of action. Eur J Pharmacol, 2014;740:364–378. Doi: 10.1016/j.ejphar.2014.07.025

7. Wang D, Lippard SJ. Cellular processing of platinum anticancer drugs. Nat Rev Drug Discov, 2005;4(4):307–320. Doi: 10.1038/nrd1691

8. Kanat O, Ertas H, Caner B. Platinum-induced neurotoxicity: a review of possible mechanisms. World J Clin Oncol, 2017;8(4):329–335. Doi: 10.5306/wjco.v8.i4.329

9. Amptoulach S, Tsavaris N. Neurotoxicity caused by the treatment with platinum analogues. Chemother Res Pract, 2011;2011(1):843019. Doi: 10.1155/2011/843019

10. Park SB, Goldstein D, Krishnan AV, Lin CS-Y, Friedlander ML, Cassidy J, et al. Chemotherapy-induced peripheral neurotoxicity: a critical analysis. CA Cancer J Clin, 2013;63(6):419–437. Doi: 10.3322/caac.21204

11. Rybak LP, Whitworth CA, Mukherjea D, Ramkumar V. Mechanisms of cisplatin-induced ototoxicity and prevention. Hear Res, 2007;226(1-2):157–167. Doi: 10.1016/j.heares.2006.09.015

12. Sham NFR, Hasani NAH, Hasan N, Karim MKA, Fuad SBSA, Hasbullah HH, et al. Acquired radioresistance in EMT6 mouse mammary carcinoma cell line is mediated by CTLA-4 and PD-1 through JAK/STAT/PI3K pathway. Sci Rep, 2023;13:3108. Doi: 10.1038/s41598-023-29925-x

13. Mosmann T. Rapid colorimetric assay for cellular growth and survival: application to proliferation and cytotoxicity assays. J Immunol Methods, 1983;65(1-2):55–63. Doi: 10.1016/0022-1759(83)90303-4

14. English K, Shepherd A, Uzor N-E, Trinh R, Kavelaars A, Heijnen CJ. Astrocytes rescue neuronal health after cisplatin treatment through mitochondrial transfer. Acta Neuropathol Commun, 2020;8(1):36 Doi: 10.1186/s40478-020-00897-7

15. Seigers R, Fardell JE. Neurobiological basis of chemotherapy-induced cognitive impairment: a review of rodent research. Neurosci Biobehav Rev, 2011;35(3):729–741. Doi: 10.1016/j.neubiorev.2010.09.006

16. Konat GW, Kraszpulski M, James I, Zhang HT, Abraham J. Cognitive dysfunction induced by chronic administration of common cancer chemotherapeutics in rats. Metab Brain Dis, 2008;23(3):325–333. Doi: 10.1007/s11011-008-9100-y

17. Patai R, Csik B, Nyul-Toth A, Gulej R, Vali Kordestan K, Chandragiri SS, et al. Persisting blood–brain barrier disruption following cisplatin treatment in a mouse model of chemotherapy-associated cognitive impairment. GeroScience, 2025;47(3):3835–3847. Doi: 10.1007/s11357-025-01569-x

18. Lomeli N, Di K, Czerniawski J, Guzowski JF, Bota DA. Cisplatin-induced mitochondrial dysfunction is associated with impaired cognitive function in rats. Free Radic Biol Med, 2017;102:274–286. Doi: 10.1016/j.freeradbiomed.2016.11.046

19. Attia A, Matta C, ElMazoudy R, Khalifa H. Cisplatin-induced neurotoxicity in cerebellar cortex of male mice involves oxidative stress and histopathology. J Basic Appl Zool, 2021;82:23. Doi: 10.1186/s41936-021-00220-3

20. Rashid MA, Oliveros A, Kim YS, Jang M-H. Nicotinamide mononucleotide prevents cisplatin-induced mitochondrial defects in cortical neurons derived from human induced pluripotent stem cells. Brain Plast, 2022;8(2):143–152. Doi: 10.3233/BPL-220143

21. Tangpong J, Cole MP, Sultana R, Joshi G, Estus S, Vore M, et al. Adriamycin-induced, TNF-α-mediated central nervous system toxicity. Neurobiol Dis, 2006;23(1):127–139. Doi: 10.1016/j.nbd.2006.02.013

22. Kann O, Kovács R. Mitochondria and neuronal activity. Am J Physiol Cell Physiol, 2007;292(2):C641–C657. Doi: 10.1152/ajpcell.00222.2006

23. Nicholls DG, Budd SL. Mitochondria and neuronal survival. Physiol Rev, 2000;80(1):315–360. Doi: 10.1152/physrev.2000.80.1.315

24. Dietrich J, Han R, Yang Y, Mayer-Pröschel M, Noble M. CNS progenitor cells and oligodendrocytes are targets of chemotherapeutic agents *in vitro* and *in vivo*. J Biol, 2006;5(7):22. Doi: 10.1186/jbiol50

25. Hui KK, Latif M, Soeandy CD, Huang S, Rodgers CE, Elia AJ, Henderson JT. Cisplatin toxicity in the developing brain displays an absolute requirement for caspase-3. Exp Neurol, 2022;351:114010. Doi: 10.1016/j.expneurol.2022.114010

26. Alotaibi M, Al-Aqil F, Alqahtani F, Alanazi M, Nadeem A, Ahmad SF, et al. Alleviation of cisplatin-induced neuropathic pain, neuronal apoptosis, and systemic inflammation in mice by rapamycin. Front Aging Neurosci, 2022;14:891593. Doi: 10.3389/fnagi.2022.891593

27. Rathinam R, Ghosh S, Neumann WL, Jamesdaniel S. Cisplatin-induced apoptosis in auditory, renal, and neuronal cells is associated with nitration and downregulation of LMO4. Cell Death Discov, 2015;1:15052. Doi: 10.1038/cddiscovery.2015.52

28. Dringen R, Gutterer JM, Hirrlinger J. Glutathione metabolism in brain. Eur J Biochem, 2000;267(16):4912–4916. Doi: 10.1046/j.1432-1327.2000.01597.x

29. Cory S, Adams JM. The BCL2 family: regulators of the cellular life-or-death switch. Nat Rev Cancer, 2002;2(9):647–656. Doi: 10.1038/nrc883

30. Youle RJ, Strasser A. The BCL-2 protein family: opposing activities that mediate cell death. Nat Rev Mol Cell Biol, 2008;9(1):47–59. Doi: 10.1038/nrm2308

31. Pabla N, Dong Z. Cisplatin nephrotoxicity: mechanisms and renoprotective strategies. Kidney Int, 2008;73(9):994–1007. Doi: 10.1038/sj.ki.5002786

32. Harris JJ, Jolivet R, Attwell D. Synaptic energy use and supply. Neuron, 2012;75(5):762–777. Doi: 10.1016/j.neuron.2012.08.019

33. Mattson MP, Gleichmann M, Cheng A. Mitochondria in neuroplasticity and neurological disorders. Neuron, 2008;60(5):748–766. Doi: 10.1016/j.neuron.2008.10.010